Scientific Research Publishing

World Journal of Engineering and Technology, 2025, 13(4), 835-844
https://www.scirp.org/journal/wjet
ISSN Online: 2331-4249
ISSN Print: 2331-4222

A Liquid Metal-Based Flexible Sensor for Finger Motion Detection via Resistance Variation

Xiwen Guo[1], Jingwen Fu[1], Junxi Liu[2], Haoyang Zheng[3], Jiaming Mao[4*]

[1]Ealing International School, Dalian, China
[2]Chengdu Foreign Languages School, Chengdu, China
[3]Bachuan International High School, Chongqing, China
[4]Logistics and E-Commerce College, Zhejiang Wanli University, Ningbo, China
Email: *mao040525@163.com

How to cite this paper: Guo, X.W., Fu, J.W., Liu, J.X., Zheng, H.Y. and Mao, J.M. (2025) A Liquid Metal-Based Flexible Sensor for Finger Motion Detection via Resistance Variation. *World Journal of Engineering and Technology*, **13**, 835-844.
https://doi.org/10.4236/wjet.2025.134052

Received: September 6, 2025
Accepted: October 19, 2025
Published: October 22, 2025

Abstract

We developed a finger motion detection sensor based on liquid metal. The sensor was fabricated by sequentially preparing an AB glue mold (embedding bamboo sticks and acupuncture needles as internal structures), injecting liquid metal into a silicone tube, followed by functional testing. Performance characterization involved measuring resistance changes under different stretching positions and forces, with relatively stable data obtained through strictly repeated operations and video recording. This sensor holds potential application value in fields such as motion monitoring, human-computer interaction, and rehabilitation assessment.

Keywords

Liquid Metal, Flexible Sensor, Resistance Variation, Motion Detection

1. Introduction

In recent years, liquid metals have shown significant potential in sensor research due to their unique properties, including high electrical conductivity, fluidity, and deformability [1], making them particularly suitable for flexible and motion-responsive devices. Traditional finger motion sensors often utilize rigid materials or complex structural designs [2], which present limitations in terms of flexibility, sensitivity to subtle movements, or ease of fabrication. While existing sensors can perform basic motion detection functions, they often struggle to maintain stability during repeated measurements or fully adapt to dynamic finger movements.

The field currently faces several challenges: for instance, ensuring performance consistency during sensor fabrication, particularly technical difficulties in the

mold preparation stage. Furthermore, obtaining stable and reliable resistance data under varying stretching positions and forces remains a core challenge; data fluctuation issues must be addressed through stringent repeatable operations and auxiliary recording methods. These challenges indicate a need for further optimization of the fabrication process and the establishment of standardized testing protocols to enhance the practical value of liquid metal-based finger motion sensors.

Experimental Section

Main Experimental Materials:

1) Gallium-Indium liquid metal (core functional material).

2) Oxidized liquid metal (used to enhance sample testing performance).

3) Component A glue and Component B glue (mixed to form silicone solution).

4) Plant stems and acupuncture needles (used with silicone to form hollow channels).

Experimental Equipment and Instruments:

1) Electronic balance (for weighing Component A/B glue).

2) Heating plate (to accelerate silicone solution curing).

3) Vacuum chamber (for degassing the silicone solution).

4) Petri dish (used as a container).

Experimental Tools and Consumables:

1) Syringe (for injecting liquid metal).

2) Glass rod (for stirring and mixing Component A and B glues).

3) Tweezers (for handling samples during performance testing).

4) Wire (for connecting the liquid metal circuit for electrical performance testing).

Experimental Procedure:

1) Silicone Solution Preparation: Silicone Part A and Silicone Part B were poured into a mixing cup at a 1:1 ratio and stirred continuously with a glass rod for 15 minutes until fully homogenized. The mixture was then placed in a vacuum chamber to remove air bubbles, resulting in a bubble-free silicone solution.

2) In the fabrication of hollow channels, the pre-treated silicone solution was first poured into a petri dish and cured under initial heating conditions for one hour. After the main body of the silicone had solidified, a plant stem (or an acupuncture needle) was placed on its surface. A second layer of silicone solution was then poured to completely cover the template, followed by secondary heat curing for four hours. Once the silicone was fully cross-linked and solidified, the embedded plant stem (or acupuncture needle) was carefully removed, and the silicone block was sectioned to obtain silicone strips featuring continuous hollow channels with an internal diameter of 1 mm.

In this experiment, bamboo subfamily (Bambusoideae) stems were selected as templates due to their inherent hydrophobicity and low interfacial adhesion, which enable complete and effortless demolding without damaging the silicone structure or causing adhesion. Moreover, their naturally smooth luminal structure

facilitates the subsequent smooth injection of liquid metal, thereby ensuring the quality and performance of the fabricated microfluidic channels.

3) During the sample preparation, a gallium-indium (Ga-In) liquid metal was injected into the central channel using a syringe. Electrical wires were then connected to both ends, and the openings were sealed with hot glue to form the final sample. To ensure reliable signal generation during performance testing, a layer of liquid metal oxide was applied to the port regions. Due to the high surface tension of the liquid metal, spherical droplets tend to form at the outlets and inlets, which can compromise electrical connectivity. Coating these areas with liquid metal oxide enhances the electrical contact between the metal and the conductive silver paste, thereby improving signal stability.

4) Performance Testing: The initial resistance of the sample was measured using an Agilent testing system. Subsequently, different parts of the sample were clamped with tweezers, and the variation in resistance over time was monitored and recorded in real time to obtain dynamic resistance response data. Finally, the collected data were analyzed and visualized using Origin software.

2. Results and Discussion

2.1. Preparation Stage and Material Selection

Liquid metal was selected as the primary conductive material. Liquid metal exhibits excellent flexibility characteristics: it typically remains liquid at room temperature, can withstand large degrees of deformation such as stretching and compression, and is resistant to permanent plastic deformation. As a metal, liquid metal possesses high electrical conductivity, nearly comparable to traditional metals, which helps ensure efficient and sensitive signal transmission. Consequently, during deformation of the liquid metal, its resistance changes correspondingly, thereby converting mechanical signals into electrical signals, which facilitates computer data acquisition and analysis. Compared to previously used mercury, liquid metal is less toxic [3] and poses minimal harm to the human body even with prolonged use.

Silicone was selected as the mold material primarily due to its excellent process adaptability and compatibility with the liquid metal injection process [4]. As shown in **Figure 1**, silicone can be rapidly poured and cured at room temperature. It has low requirements for master mold materials (metal acupuncture needles, bamboo branches, etc., can all serve as master molds), making it particularly suitable for small-batch trial production or personalized sensor fabrication, with high operational convenience. Silicone is soft, exhibits low surface tension, and possesses certain elasticity, making it easy to demold after curing, thereby significantly improving manufacturing success rates. During the molding process, silicone closely adheres to the mold cavity, effectively preventing leakage of the injected liquid metal and ensuring complete filling of the cavity (as illustrated by the injection process in **Figure 1**). The surface of the cured silicone mold is smooth, which significantly reduces friction resistance with the liquid metal and avoids adverse effects on the sensor's electrical performance due to surface imperfections.

Figure 1. The arrow indicates the direction of liquid metal injection.

The operating principle of the sensor is based on a resistance sensing mechanism [5] correlated with its deformation capability. The relative change in electrical resistance ($\Delta R/R_0$) of the sensor during stretching is given by the following formula:

$$\frac{\Delta R}{R_0} = \varepsilon^2 + 2\varepsilon$$

where ΔR and R_0 represent the change in electrical resistance after stretching and the initial resistance value in the relaxed state, respectively, and ε denotes the strain applied to the sensor. According to the characteristics of the piano curve-type liquid metal structure under transverse or longitudinal stretching, its internal structure begins to deform initially from the outermost pattern, while the sub-outer layer remains unchanged. As the stretching amount increases, the pattern deformation progressively transmits from the outer to the inner layers, resulting in a steady increase in resistance. This structure prevents the rupture of the liquid metal structure caused by localized excessive deformation, thereby endowing the sensor with excellent isotropic stretching characteristics.

2.2. Mechanical and Electrical Properties of the Sensor

Figure 2. The lower section indicates the sensor's length in the relaxed state; the upper section demonstrates its length change under stretching.

Gallium-based liquid metals exhibit significant characteristics in terms of electrical resistivity variation with temperature [6]. Experimental results demonstrate that within the physiological temperature range from room temperature to 45˚C (encompassing typical hand temperatures of 30˚C - 37˚C), the electrical resistivity of liquid metal decreases linearly with increasing temperature. Hand temperature is transmitted to the liquid metal microchannels within the sensor via thermal conduction, triggering thermal expansion effects and resistivity changes in the liquid metal: rising temperature causes volume expansion of the liquid metal, increasing the conductive cross-sectional area within the microchannels and thereby

reducing electrical resistance. These electrical characteristic variations directly lead to fluctuations in the sensor's resistance signals due to changes in finger temperature. Similar findings have been reported in studies on stretchable nanoparticle conductors with self-organized conductive pathways [7]. Simultaneously, the change in electrical resistivity caused by temperature superimposes with the resistance variation resulting from mechanical deformation (such as tension or compression), thereby introducing additional errors into the force sensing signal. These electrical characteristics directly lead to fluctuations in the sensor's resistance signal due to changes in finger temperature. As shown in **Figure 2**, structural deformation occurs in the sensor under mechanical stretching, which alters the geometry of the conductive path (e.g., increased length and reduced cross-sectional area), thereby modulating the resistance value.

Meanwhile, compared to manual manipulation, tweezers provide a more precise and stable method of applying force. Liquid metal sensors typically require highly controlled stretching conditions, necessitating precise control over both the magnitude and direction of stretch. During manual stretching, hand muscles struggle to apply minute and stable forces, easily leading to uneven stretching and adversely affecting sensor performance testing. As shown in **Figure 3**, Tweezers allow for precise gripping of specific parts of the sensor, enabling stretching operations with minute and stable forces, which facilitates accurate acquisition of performance data under various deformation states. Prolonged manual operation is prone to tremors due to external factors, which is detrimental to the precise stretching experiments required for liquid metal sensors. Tweezers, often featuring lightweight design and anti-slip treatment, can mitigate the impact of hand tremors on the sensor stretching process, ensuring smooth operation and thereby enhancing the reliability of test data.

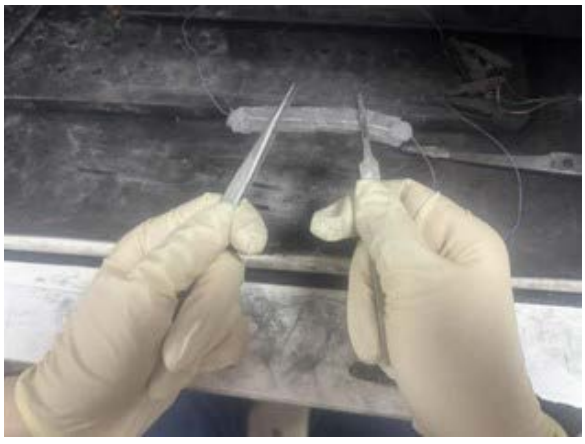

Figure 3. Schematic illustration of the practical stretching operation using laboratory tweezers.

The successfully fabricated liquid metal sensor was connected to a computer and subjected to stretching tests. Recorded data were processed using Origin software. Observation revealed that the rate of resistance change exhibited a gradual

upward trend with increasing stretch ratio.

For the first-generation liquid metal sensor, I used a liquid metal sensor mold made of acupuncture needles, which had a smaller cross-sectional area and a narrower channel for filling liquid metal inside. For the second-generation liquid metal sensor, we use a liquid metal sensor mold made from plant stems, which has a larger cross-sectional area and a wider channel for filling the liquid metal sensor inside.

The sensor we produce is a tensile sensor. Its basic principle is that when the sensor is stretched or bent, the liquid metal channel inside is elongated, and at the same time, its cross-sectional area decreases. As the length increases and the cross-sectional area decreases, the superposition of these two effects causes the total resistance to increase significantly with deformation. The rate of change in resistance is a measure of this sensitivity. Under the premise that other conditions (length, height, liquid metal material) are the same, the cross-sectional area of the wide channel is larger and the initial resistance value is smaller. After being stretched to the same length, the width and height of the channel decrease in the same ratio. For narrow channels, the initial cross-sectional area is small, and the same deformation will lead to a greater relative rate of change in the cross-sectional area. For wide channels, the initial cross-sectional area is larger. The same deformation will result in a smaller relative change rate of the cross-sectional area.

The Poisson effect also explains this phenomenon [8]. The Poisson effect indicates that when a material is stretched in one direction, it will contract in two other directions perpendicular to the stretching direction. Poisson's ratio is a material constant, which is the negative ratio of lateral strain to axial strain. In our liquid metal sensor, when the silicone mold is stretched, the internal liquid metal channels are also stretched. Axial strain is caused by the external force manually applied during the stretching process, while lateral strain is due to the Poisson effect, which is the contraction of the channel in both the width and height directions. The change in cross-sectional area directly determines the change in resistance value. The larger the Poisson's ratio is, the more severe the area reduction will be and the more obvious the change in resistance value will be.

In conclusion, as can be seen from **Figure 4**, the first-generation liquid metal sensor can test more precise and obvious change values and can be used to detect some subtle changes [9]. Meanwhile, the data in **Figure 5** and **Figure 6** reveal that although the second-generation liquid metal sensor is not as accurate as the first one, it is easier to demold and more convenient to manufacture, making it more suitable for daily mass production.

The working mechanism of the liquid metal (e.g., gallium-based alloys) encapsulated within the silicone substrate is as follows: during finger bending, deformation of the silicone matrix forces the internal liquid metal channel to elongate and its cross-sectional area to decrease. A larger bending angle results in a higher stretching ratio of the liquid metal, leading to a significant increase in its length (L) and a corresponding decrease in its cross-sectional area (S). According to the

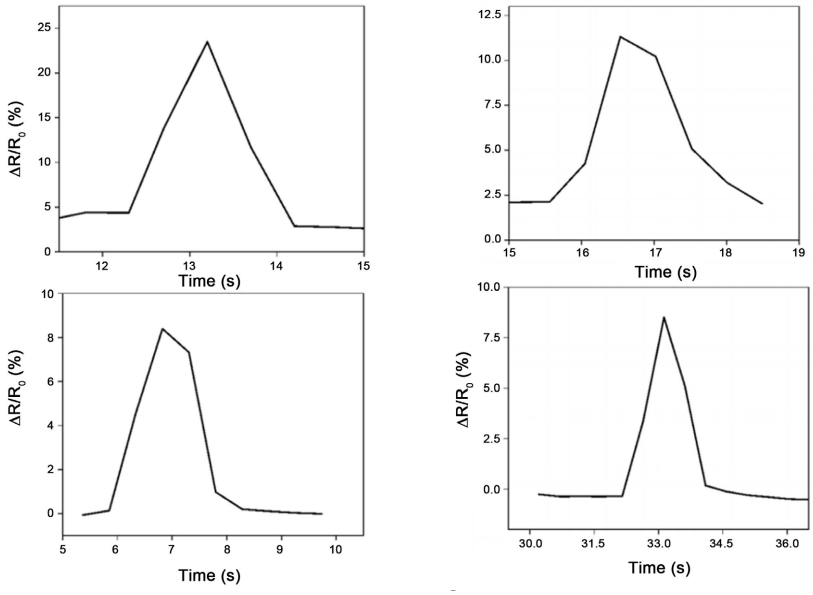

Figure 4. Performance testing results of the first-generation liquid metal sensor under stretching conditions.

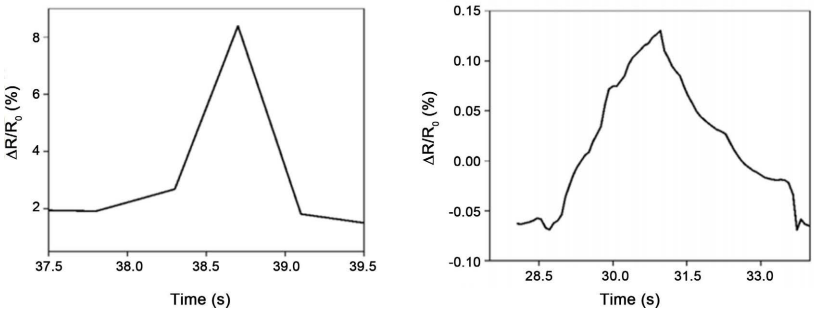

Figure 5. Schematic diagram of stretching performance testing for the second-generation liquid metal sensor.

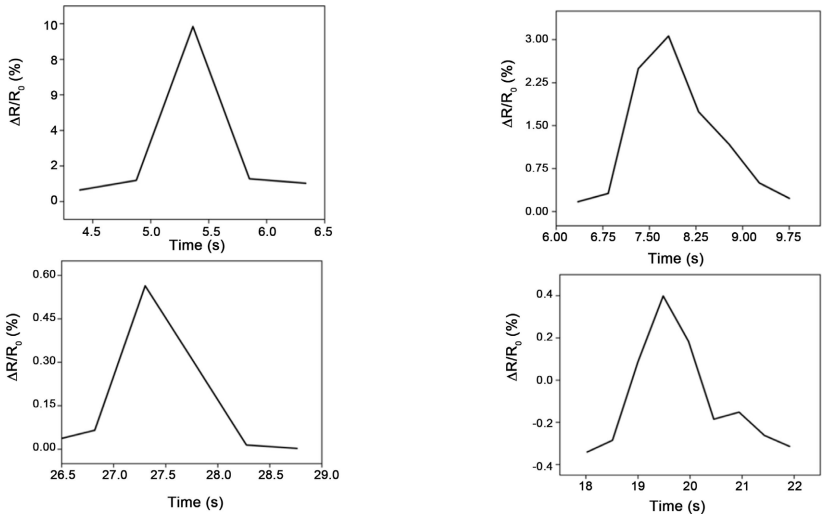

Figure 6. Schematic diagram of stretching performance testing for the second-generation liquid metal sensor.

electrical resistance law, $R = \rho L / S$ (where ρ is the resistivity), these changes collectively cause a corresponding increase in the electrical resistance (R). By precisely measuring the change in resistance, the strain level during finger bending can be derived, enabling the accurate conversion to the precise bending angle.

$$R = \rho \frac{L}{S}$$

At a constant temperature, the electrical resistance of a conductor is directly proportional to its length and inversely proportional to its cross-sectional area, while also being directly related to its resistivity (a material property). This law applies to uniform conductors and serves as the fundamental theory for analyzing changes in electrical resistance. Taking the liquid metal sensor as an example, the increase in length (L) and reduction in cross-sectional area (S) caused by stretching directly lead to a rise in electrical resistance (R) in accordance with this law.

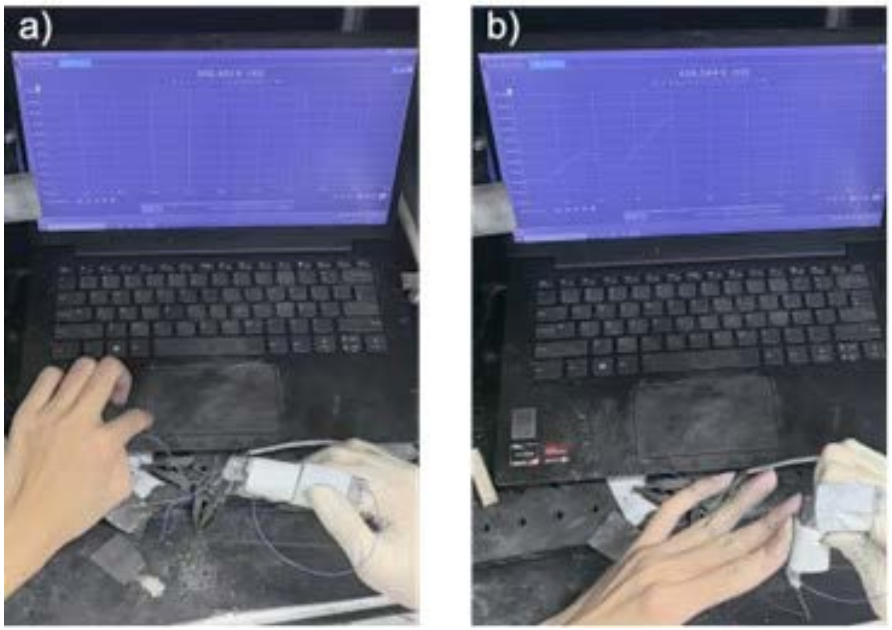

Figure 7. Schematic diagram of resistance change measurement during finger bending experiments in laboratory setting.

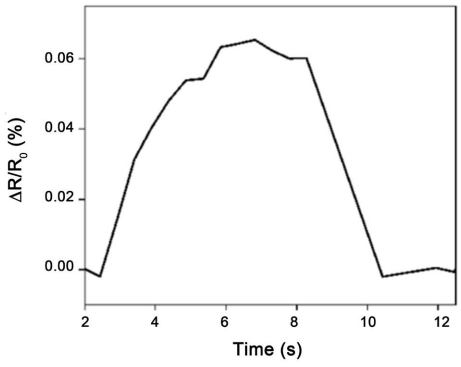

Figure 8. Finger bent at 30 degrees.

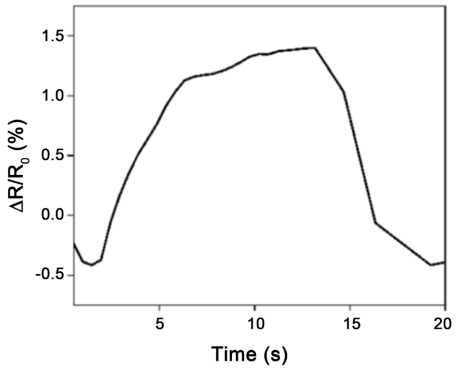

Figure 9. Finger bent at 60 degrees.

As shown in the schematic diagram of resistance change measurement during finger bending experiments (**Figure 7**), the electrical resistance of the sensor changes correspondingly with finger extension and flexion movements. For instance, when the finger is bent at 30 degrees (**Figure 8**) or 60 degrees (**Figure 9**), the resistance varies predictably due to the strain-induced changes in the conductive material. When the finger returns to its original position, the resistance value also reverts to its baseline level. Leveraging this characteristic, we can utilize the sensor to distinguish repetitive bending actions of the knee joint with different amplitudes and frequencies, demonstrating its significant potential for applications in the field of human-computer interaction.

3. Conclusions

In this study, a metal casting method was primarily employed for sensor fabrication: a mold was pre-prepared, followed by injection of liquid gallium-zinc alloy into it, with electrodes embedded on both sides to produce finger motion sensors. By repeating this process, multiple fully functional samples were successfully fabricated. The sensor operates by detecting changes in resistance corresponding to various finger bending angles, enabling precise tracking of human finger movements. Through analysis of the collected data, the sensor demonstrated its capability to monitor human motion states when attached to different joints.

Future work will focus on enhancing the portability of the sensor and advancing its applications in the medical field. Specifically, it could assist patients in rehabilitation training by allowing healthcare professionals to monitor the quality and progress of exercises. Additionally, owing to its wide deformation tolerance, high repeatability, and excellent dynamic response, this type of sensor shows significant potential for applications in soft robotics [10].

Conflicts of Interest

The authors declare no conflicts of interest regarding the publication of this paper.

References

[1] Xun, Y.H., Zhang, Z., Fan, W.C., *et al.* (2022) Design of a Flexible Bending Sensor

with Large Deformation Based on Liquid Metal. *Instrument Technique and Sensor*, No. 6, 6.

[2] Sun, Y., Wang, Z.S., Han, Z.H., *et al.* (2023) Design Optimization and Experimental Verification of a Gallium-Based Liquid Metal Flexible Strain Sensor. *Journal of Instrumentation*, **44**, 16-26.

[3] Qi, Y., Tan, B., Zhu, R., Li, D., Liu, S. and Chen, X. (2025) Liquid Metal Composites for Wearable Healthcare Sensors. *Rare Metals*, **44**, 5980-6001. https://doi.org/10.1007/s12598-025-03335-6

[4] Zhang, Q. (2020) Research on Flexible Pressure Sensor Based on Liquid Metal. Master's Thesis, Shenzhen University.

[5] Tang, Y.D. and Luo, Y.L. (2022) A Peano Curve-Type Liquid Metal Strain Sensor and Its Preparation Method. Invention Patent Application CN 115479533 A.

[6] Wang, Y.C., Lu, Y.T., Mei, D.Q. and Zhu, L.F. (2021) Liquid Metal-Based Wearable Tactile Sensor for Both Temperature and Contact Force Sensing. *IEEE Sensors Journal*, **21**, 1694-1703.

[7] Kim, Y., Zhu, J., Yeom, B., Di Prima, M., Su, X., Kim, J., *et al.* (2013) Stretchable Nanoparticle Conductors with Self-Organized Conductive Pathways. *Nature*, **500**, 59-63. https://doi.org/10.1038/nature12401

[8] Park, Y., Majidi, C., Kramer, R., Bérard, P. and Wood, R.J. (2010) Hyperelastic Pressure Sensing with a Liquid-Embedded Elastomer. *Journal of Micromechanics and Microengineering*, **20**, Article ID: 125029. https://doi.org/10.1088/0960-1317/20/12/125029

[9] Wu, Y.Z., Zhou, Y.L., Asghar, W., Liu, Y.W., Li, F.L., Sun, D.D., *et al.* (2021) Liquid Metal-Based Strain Sensor with Ultralow Detection Limit for Human-Machine Interface Applications. *Advanced Intelligent Systems*, **2021**, Article ID: 2000235.

[10] Boley, J.W., White, E.L., Chiu, G.T. and Kramer, R.K. (2014) Direct Writing of Gallium-Indium Alloy for Stretchable Electronics. *Advanced Functional Materials*, **24**, 3501-3507. https://doi.org/10.1002/adfm.201303220